VOL. 18, NO. 14, JULY 2023 ISSN 1819-6608
ARPN Journal of Engineering and Applied Sciences

www.arpnjournals.com

PULSE OXIMETER IMPLEMENTED WITH ESP32 AND MONITORED IN BLYNK AND THINKSPEAK

Julián R. Camargo L., Oscar D. Flórez C. and Adolfo Andrés Jaramillo-Matta
Faculty of Engineering, Universidad Distrital Francisco José de Caldas, Bogotá D. C., Colombia
E-Mail: jcamargo@udistrital.edu.co

ABSTRACT

Before the COVID-19 pandemic, pulse oximeters were commonly used in clinics, hospitals, medical centers, and homes of individuals requiring a prescription. As a result of the health crisis caused by COVID-19, their use has been normalized and they can now be found in the first aid kit of many homes along with the thermometer. This article shows the design and experimental implementation of a pulse oximeter using an ESP32 microcontroller that allows through its Bluetooth and WiFi modules to perform an IoT (Internet of Things) application in conjunction with the online platform ThingSpeak and the Android application Blynk, generating remote and real-time monitoring of the information generated by a sensor that can measure blood oxygen concentration and heart rate reference MAX30102.

Keywords: blynk, ESP32, pulse oximeter, SpO_2, ThingSpeak.

Manuscript Received 20 April 2023; Revised 17 September 2023; Published 30 September 2023

1. INTRODUCTION

Pulse oximetry is a noninvasive method that allows the estimation of arterial hemoglobin oxygen saturation and also evaluates heart rate and pulse amplitude. The partial pressure of dissolved oxygen in arterial blood is called PaO_2. The percentage saturation of oxygen bound to hemoglobin in arterial blood is called SaO_2 and when measured by a pulse oximeter, this value is called SpO_2. [1] Pulse oximetry is the difference in the absorption of light waves by oxygenated and deoxygenated hemoglobin.

The oximeter has a diode that emits red to near-infrared light waves with a photodiode at the other end that detects the light transmitted or reflected through the tissue and a microprocessor that can identify and separate the pulsatile (arterial) from the non-pulsatile (venous) component, and according to the absorption of the light waves calculate the arterial oxygen saturation (SaO_2) of the pulsatile (arterial) hemoglobin using the average of repeated measurements over some time. The result is the percentage oxygen saturation of arterial blood hemoglobin (SaO_2). When measured with the pulse oximeter, it is called SpO_2, in addition to the number of beats that informs the heart rate per minute. [2]

The ability of the pulse oximeter to detect arterial blood SpO_2 is based on the fact that the amount of red and IR light absorbed fluctuates with the cardiac cycle, as arterial blood volume increases during systole and decreases during diastole; in contrast, blood volume in veins and capillaries remains relatively constant. A portion of the light that passes through the tissues without being absorbed is incident on the photodetector, creating signals with a relatively stable, non-pulsating direct current (DC) component and a pulsating alternating current (AC) component (Figure-1A).

A cross-sectional diagram of an artery and vein during systole and diastole illustrates the non-pulsatile (DC) and pulsatile (AC) compartments of arteries and the relative absence of volume change in veins and capillaries (Figure-1B). Pulse oximeters use the amplitude of the absorbances to calculate the red: IR (R) modulation ratio (1) [3]:

$$R = \frac{A_{red,AC}/A_{red,DC}}{A_{IR,AC}/A_{IR,DC}} \quad (1)$$

Where A = absorbance, R is a twofold ratio of the pulsatile and non-pulsatile components of red light absorption to IR light absorption.

At low arterial oxygen saturations, where there is an increase in HHb, the relative change in the amplitude of the red light absorbance due to the pulse is greater than the IR light absorbance, i.e., $A_{red,AC} > A_{IR,AC,}$ resulting in a higher R-value; conversely, at higher oxygen saturations, $A_{IR,AC} > A_{red,AC}$ and the R value is lower (Figure-1C).

The pulse oximeters' microprocessor uses this relationship (calculated over a series of pulses) to determine SpO_2 based on a calibration curve generated empirically by measuring R in healthy volunteers whose saturations were altered from 100% to approximately 70%. (Figure-1C).

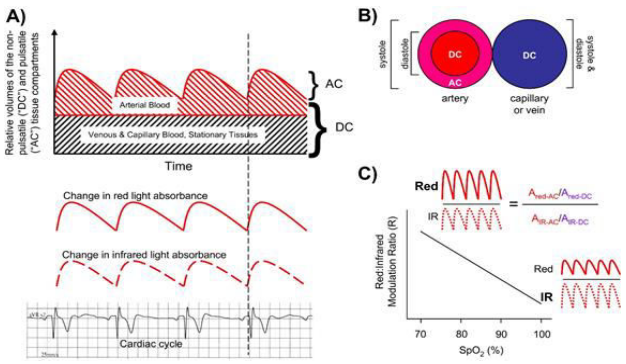

Figure-1. Schematic diagram of light absorbance by a pulse oximeter [3].

Therefore, SpO2 readings below 70% should not be considered quantitatively reliable, although it is unlikely that clinical decisions would be altered based on differences in measured SpO2 below 70%. [3]

The way pulse oximeters exclude the influence of venous and capillary blood and other stationary tissues from the SpO_2 calculation is based on the Beer-Lambert Law of absorbance applied to a modeled blood vessel as seen in (2):

$$A = \varepsilon bc \tag{2}$$

Where A = absorbance, ε = absorption (or extinction) coefficient of hemoglobin at a specific wavelength (a combination of the O_2Hb and HHb coefficients), b = path length of light emitted through the blood vessel, and c = Hb concentration.

Absolute absorbance measurement is an inaccurate estimate of arterial SpO_2, as elevated HHb levels in venous blood also contribute to the measured value. However, a pulse oximeter can only determine arterial SpO_2 by measuring absorbance changes over time [3]. Mathematically the total absorbance (A_t) can be considered as a linear combination of the venous (A_v) and arterial (A_a) absorbances as shown in (3):

$$A_t = A_v + A_a = \varepsilon_v b_v c_v + \varepsilon_a b_a c_a \tag{3}$$

Since pulse oximeters measure absorbance concerning time, the derivative of the above equation becomes (4):

$$\frac{dA_t}{dt} = \frac{d(\varepsilon_v b_v c_v)}{dt} + \frac{d(\varepsilon_a b_a c_a)}{dt} \tag{4}$$

Because ε and c are constants, equation (4) simplifies to (5):

$$\frac{dA_t}{dt} = \frac{db_v}{dt}(\varepsilon_v c_v) + \frac{db_a}{dt}(\varepsilon_a c_a) \tag{5}$$

As the arteries dilate and contract much more than the veins, i.e., the change in $b_a \gg$ the change in b_v ($db_a/dt \gg db_v/dt$), one can assume b_v as a constant and $db_v/dt = 0$; therefore, equation (5) simplifies to (6):

$$\frac{dA_t}{dt} = \frac{db_a}{dt}(\varepsilon_a c_a) \tag{6}$$

This is summarized as $\Delta A_t = \Delta A_a$, which means that the change in A_t measured = change in absorbance due to arterial blood content with little or no contribution from venous blood. Therefore, an adequate pulse is necessary for pulse oximeters to function, so attempting to measure SpO_2 in regions with little or no blood perfusion will result in absent or inaccurate readings. [3]

The pulse oximeter is used to determine blood oxygen levels noninvasively, to monitor patients with respiratory problems [4], to perform sleep studies (and detect cases of obstructive sleep apnea), to detect a priori cases of COVID-19 in asymptomatic patients [5]- [6], to detect secondary problems generated by COVID-19 [7], for sports practice, among others.

To implement a pulse oximeter at a practical level, we can use a commercial reference sensor MAX30102 (measures blood oxygen concentration and heart rate), belonging to the MAX3010x family [8], which, as required by a commercial pulse oximeter, emits red and infrared light. Employing the information reflected in the blood, we obtain (utilizing an algorithm) the percentage of oxygen saturation and a value of the number of beats per minute emitted by the heart. The light reflected by the blood is the input of the algorithm that, employing an internal analog-to-digital converter (ADC) and signal processing, is transformed into the required medical data; this information is available to be sent to the outside through the I^2C protocol.

This paper presents the design and implementation of a pulse oximeter [9]- [16] that makes use of the MAX30102 sensor that will measure blood oxygen concentration and heart rate [17]- [20], an ESP32 microcontroller [19], a 128 x 128-pixel color graphic LCD, where the pulse oximeter information will be displayed locally [20]- [22] and a remote display system implemented in Blynk and ThingSpeak.

2. SOLUTION DESIGN AND MODEL

2.1 Hardware

The hardware configuration shown in Figure-2 is proposed, which includes as a central device the ESP32 microcontroller (in charge of all the control and processing of the system), which will be connected to the MAX30102 sensor through an I^2C communications port and to a graphic LCD through an SPI port (to visualize the data taken from the sensor locally). For the remote visualization of the data, a smartphone will be used, which will communicate via Bluetooth with the ESP32 and using the WiFi module, will connect via Web to the free API ThingSpeak.

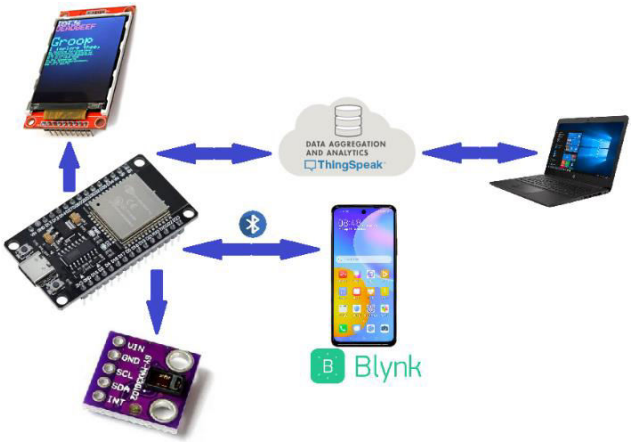

Figure-2. Diagram of the proposed system design

2.2. Types of Total Capacity Control

The general algorithm for solving the problem is implemented in the ESP32 memory and is based on the flowchart shown in Figure-3.

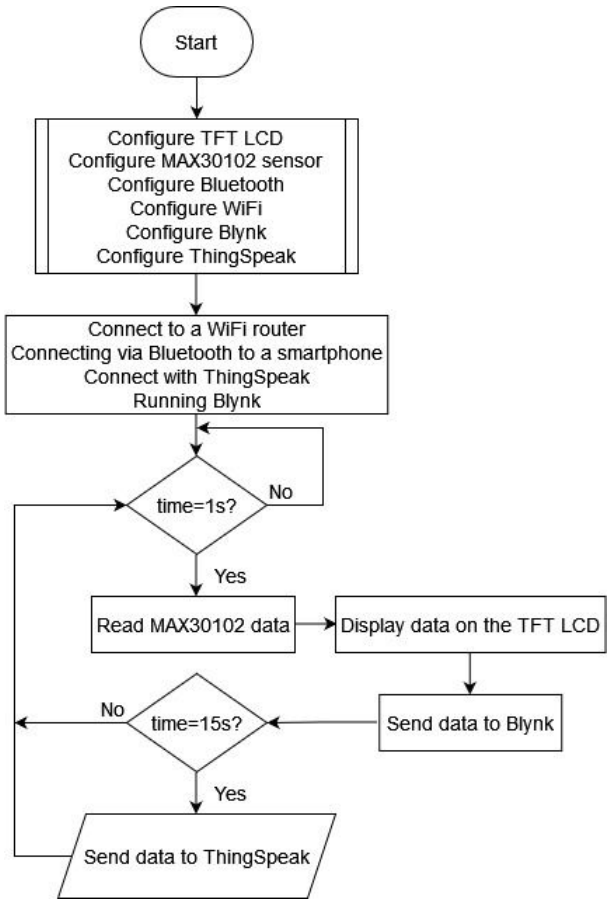

Figure-3. General flow diagram.

The first task in the algorithm is the configuration of the elements included in the design; in all cases, libraries provided officially by the manufacturer of each of the components are used: for the TFT LCD, the library *TFT_ILI9163C.h* together with the graphic library *Adafruit_GFX.h*, for the MAX30102 sensor the library *MAX30105.h* library that operates for the whole MAX3010x sensor family, for Bluetooth the *BLEDevice.h* and *BLEServer.h* libraries, for WiFi the *WiFi.h* and *WiFiClient.h* libraries, for Blynk the *BlynkSimpleEsp32_BLE.h* library and finally for the connection with ThingSpeak the *ThingSpeak.h* library.

The next step in the process is to connect to the previously configured WiFi access point, connect the internal Bluetooth module with the Bluetooth of the smartphone and finally connect to Blynk and ThingSpeak.

Then we have two processes one is repeated once per second (sending data to Blynk) called *sendToBlynk()* and the other every 15 seconds (sending data to ThingSpeak) called *sendToThingSpeak()*; the code implemented in the Arduino IDE for both cases can be seen in Figure-4.

The data sent in both processes correspond to beats per minute (*beatsPerMinute*), average beats (*beatAvg*), beats per second (*beatsPerSecond*) and oxygen saturation SpO_2 (*oxygen*).

Figure-4. sendToThingSpeak() and sendToBlynk() Functions.

2.3 Design in Blynk

Blynk is a platform for IoT. Blynk allows controlling an app using a microcontroller and an iOS or Android device. Using Blynk, the user can create a graphic interface of “drag and drop”. This application is focused on platforms like Arduino, Raspberry Pi, ESP32, Intel Galileo, serial devices, and WiFi. [23]- [25]

The designed app can be seen in Figure-5, the task performed in the app is to collect and visualize the information on oxygen saturation, beats per minute, average beats per minute and beats per second, sent by the ESP32 via Bluetooth. These values are displayed in the app in graphical form (in a gauge, a horizontal bar, a vertical bar and a graph over time) and as numerical values.

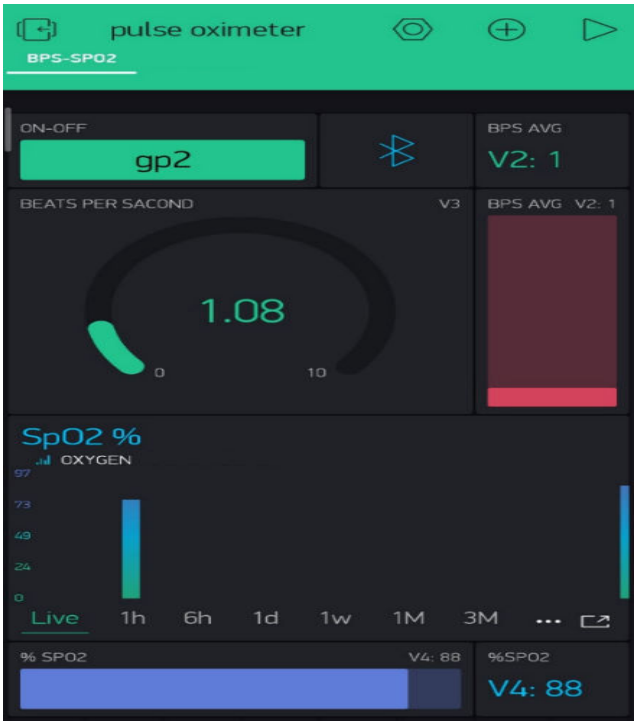

Figure-5. Data visualization in Blynk.

2.4 Configuration and Start-Up of the ThingSpeak Platform

ThingSpeak is an API for development in the field of the Internet of Things (IoT); it allows storing and collecting data from objects connected via the HTTP protocol through the Internet or a local network; the configuration of this API is quite intuitive and straightforward, the user needs to create an account in MathWork (the same developer of MatLab) through an active email, once this is done, proceed to create a channel and the application is ready to run immediately by linking the channel name to the application being developed.

Part of the configuration of the channel created in ThingSpeak (enabling fields) for developing the pulse oximeter is shown in Figure-6.

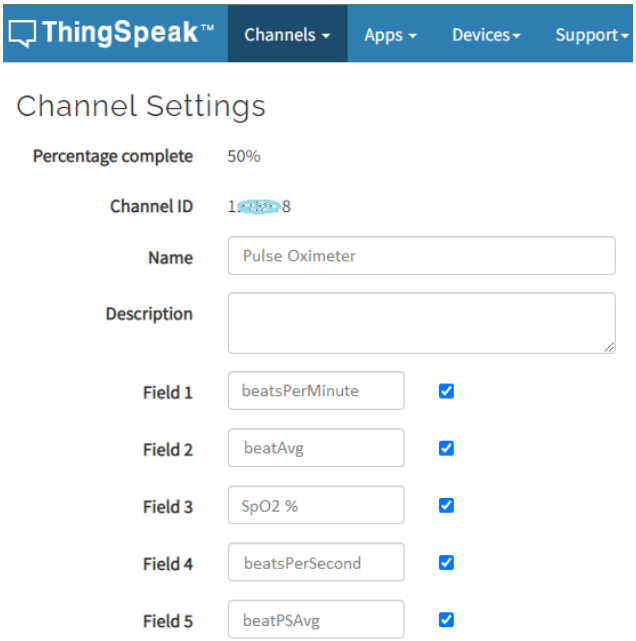

Figure-6. Channel configuration in ThingSpeak.

3. RESULTS

A study in Colombia evaluated SaO2 in 264 healthy men and women between 18 and 30 years at altitudes between 970 m and 2600 m above sea level (Table-1), finding few differences, but being lower at 2600 m (average SaO2 men 93.6% vs. 94.8% women 93.6% vs. 96.4%).

Table-1. Arterial oxygen saturation at different altitudes in healthy populations in Colombia [2].

Altitude over sea level	SaO_2 % Men Mean (IC95%)	SaO_2% Women Mean (IC95%)
970mt	94,8 (94,1-95,4)	96,4 (95,7 – 97,1)
1520	95,5 (94,9-96,1)	95,6 (94,9 – 96,2)
1728	95,7 (95,3-96,2)	96,1 (95,6 – 96,6)
1923	95,1 (94,3-95,8)	96 (95,6-96,3)
2180	95,2 (94,6-95,9)	95,4 (94,9-95,9)
2600	93,6 (93,2-94)	94,4 (94,1-94,8)

In Bogota, arterial oxygen pressure (PaO2) can go from 68-70 mmHg in children under 30 years to 62-60 mmHg in men and women over 70 years, corresponding to a calculated SaO2 of 94% and 92%, respectively. In Medellin at 1538 m above sea level, a study of 76 healthy adults aged 20-45 years found a mean PaO2 of 80 mmHg (95%CI: 79.7-81.5) corresponding to a calculated SaO2 of 96%. [2]

In summary, the results obtained in the measurements have a direct dependence on the altitude at which the measurement equipment is located [26]- [28]; in this case, the designed device is located in the city of Bogotá (Colombia), a city located at an altitude of

2600mts, so it is necessary to take into account the results of the study shown in Table-1.

Having clarity on the expected data ranges, we tested the implemented oximeter, which can be seen in Figure-7. A commercial Oxywatch pulse oximeter with reference number 20456338 was used to contrast the results.

Figure-7. Implemented pulse oximeter.

Table-2 shows the measurement results of 15 people; in each case, ten measurements were taken simultaneously, at one-minute intervals, with the device designed and the commercial pulse oximeter. The samples' average was calculated, corresponding to the information presented in the table.

Table-2. Average measurements obtained.

Subject No.	SpO_2 (%)		Pulse rate	
	Protot.	Comm.	Protot.	Comm.
1	95	94	88	89
2	93	95	87	86
3	95	96	90	93
4	92	91	105	108
5	92	93	98	97
6	94	95	95	95
7	91	90	90	92
8	95	96	95	97
9	93	92	90	93
10	90	91	98	98
11	95	93	88	87
12	96	97	92	89
13	93	94	102	101
14	94	95	107	111
15	95	94	92	90

Figure-8 shows the results obtained graphically for oxygen saturation (SpO_2 %) for both the prototype and the commercial pulse oximeter, according to the data in Table-2.

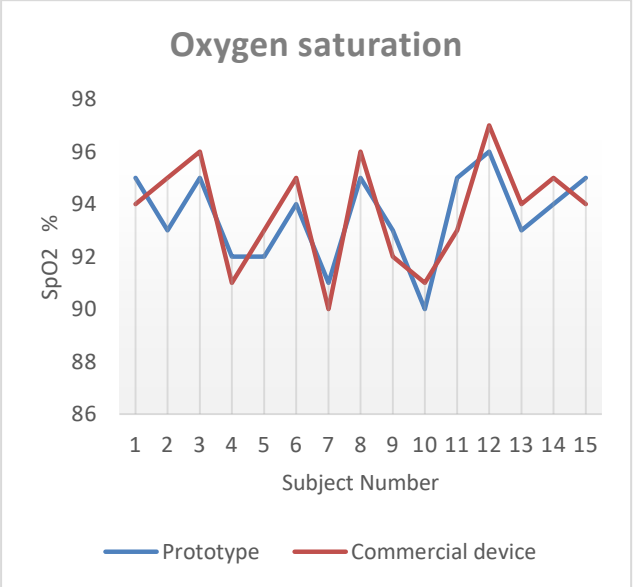

Figure-8. Oxygen saturation data comparison.

As can be seen in the graph, the differences between the values measured for oxygen saturation using the implemented prototype and the values measured by the commercial pulse oximeter have no significant differences. It can be concluded a priori that the prototype meets its objective.

In Figure-9, the results obtained for the heart rate measured in beats per minute are presented graphically, both for the prototype implemented and for the commercial pulse oximeter, according to the data previously recorded in Table-2.

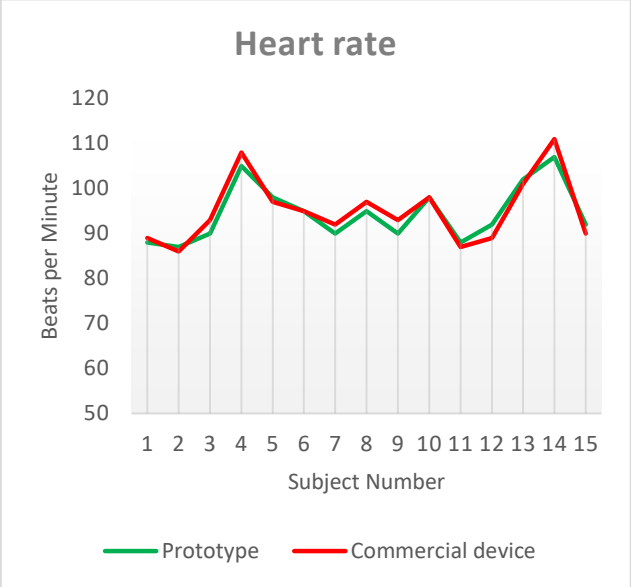

Figure-9. Heart rate data comparison.

The percentage error calculation concerning the commercial pulse oximeter is presented in Table-3, both for each subject and the overall average obtained from the 15 test subjects.

Table-3. Calculated error percentages.

Subject No.	SpO_2 error (%)	Pulse rate error (%)
1	1,064	1,124
2	2,105	1,163
3	1,042	3,226
4	1,099	2,778
5	1,075	1,031
6	1,053	0,000
7	1,111	2,174
8	1,042	2,062
9	1,087	3,226
10	1,099	0,000
11	2,151	1,149
12	1,031	3,371
13	1,064	0,990
14	1,053	3,604
15	1,064	2,222
Average error	1,209	1,875

The data sent to ThingSpek can be seen in Figure-10; these data are updated every 15 seconds because the free version, which was used, does not allow sending at shorter intervals.

Figure-10. Data visualization in ThingSpeak.

5. CONCLUSIONS

With the results obtained, it can be indicated that the proposed pulse oximeter has adequate performance, concluding that the MAX30102 sensor has a sensitivity value within the margins shown in the user's manual, making it ideal for this type of medical application.

The tests performed on the prototype show its good performance since relative error percentages (on average less than 2%.) of a meager value were found; with more exhaustive tests, the prototype could be used at a medical level.

ACKNOWLEDGMENTS

The authors would like to thank the Universidad Distrital Francisco José de Caldas and the LASER research group that supported the development and testing of the project.

REFERENCES

[1] H. Mejia-Salas and M. Mejía-Suárez. 2012. Pulse oximetry. Revista de la Sociedad Boliviana de Pediatría. 51(2): 149-155.

[2] Ministerio de Salud - Colombia. 2015. Uso e interpretación de la oximetría de pulso. [Online]. Available: https://www.minsalud.gov.co/sites/rid/Lists/BibliotecaDigital/RIDE/VS/PP/ENT/uso-interprtn-oximetria-pulso.pdf

[3] E. D. Chan, M. M. Chan and M. M. Chan. 2013. Pulse oximetry: Understanding its basic principles facilitates appreciation of its limitations. Respiratory Medicine. 107(6): 789-799.

[4] G. Tusman, S. H. Bohm and F. Suarez-Sipmann. 2017. Advanced Uses of Pulse Oximetry for Monitoring Mechanically Ventilated Patients. Anesthesia & Analgesia. 124(1): 62-71.

[5] A. Chauhan, R. Kaur, P. Chakrbarti and A. Pal. 2021. Silent Hypoxemia - Leads to Vicious Cycle of Infection, Coagulopathy and Cytokine Storm in COVID-19: Can Prophylactic Oxygen Therapy Prevent It?. Indian Journal of Clinical Biochemistry. 36(4): 468-472.

[6] T. S. Simonson, T. L. Baker, R. B. Banzett, T. Bishop, J. A. Dempsey, J. L. Feldman, P. G. Guyenet, E. J. Hodson, et al. 2021. Silent hypoxaemia in COVID-19 patients. The Journal of Physiology. 599(4): 1057-1065.

[7] C. Shi, M. Goodall, J. Dumville, J. Hill, G. Norman, O. Hamer, et al., "The accuracy of pulse oximetry in measuring oxygen saturation by levels of skin pigmentation: a systematic review and meta-analysis," BMC Medicine, vol. 20, pp. 2-14, 2022.

[8] R. Suhartina and T. Abuzairi. 2021. Pulse Oximeter Monitoring Bracelet for COVID-19 Patient using Seeeduino. Jurnal Ilmiah Teknik Elektro Komputer dan Informatika. 7(1): 81-87.

[9] H. Sebestova, S. Walzel and P. Kudrna. 2022. Educational Pulse Oximeter Controlled by Microprocessor. 2022 E-Health and Bioengineering Conference (EHB), Iasi, Romania. pp. 1-4.

[10] A. Keerthika and R. Ganesan. 2013. Pervasive Health Care System for Monitoring Oxygen Saturation using Pulse Oximeter Sensor. 2013 IEEE Conference on Information & Communication Technologies, Thuckalay, India. pp. 819-823.

[11] R. K. Parate, K. M. Dhole, S. J. Sharma. 2023. Design of a Node-MCU based Web-Server for Heart rate and SpO2 Monitoring. International Journal of Engineering Research & Technology. 12(1): 58-61.

[12] L. Mennicke and K. Hofmann. 2021. .Pulse Oximetry - Teaching basic Electronic Sensor Signal Processing in a Medical Context. 2021 IEEE Frontiers in Education Conference (FIE), Lincoln, NE, USA. pp. 1-4.

[13] P. P. Banik, S. Hossain, T.-H. Kwon, H. Kim and K.-D. Kim. 2020. Development of a Wearable Reflection-Type Pulse Oximeter System to Acquire Clean PPG Signals and Measure Pulse Rate and SpO2 with and without Finger Motion. Electronics. 9(11): 1-26.

[14] G. Bucci, F. Ciancetta, E. Fiorucci, A. Fioravanti and A. Prudenzi. 2019. A Pulse Oximetry IoT System Based on Powerline Technology. 2019 II Workshop on Metrology for Industry 4.0 and IoT (MetroInd4.0&IoT), Naples, Italy. pp. 268-273.

[15] T. J. Jeyaprabha, A. Abijith, G. Prashanth and T. Chiranjeevraja. 2019. Implementation of remote patient monitoring using wireless pulse oximeter. International Journal of Recent Technology and Engineering. 7(5): 458-463.

[16] G. Ateş and K. Polat. 2012. Measuring of oxygen saturation using pulse oximeter based on fuzzy logic. 2012 IEEE International Symposium on Medical Measurements and Applications Proceedings, Budapest, Hungary. pp. 1-6.

[17] R. Wahyuni, Herianto, Ikhtiyaruddin and Y. Irawan. 2023. IoT-Based Pulse Oximetry Design as Early Detection of Covid-19 Symptoms. International Journal of Interactive Mobile Technologies. 17(3): 177-187.

[18] W. F. Bastari, M. A. Anshori and M. R. Ramadhani. 2022. Design &Construction of Oxygen Saturation Measuring Equipment through the Thingspeak Server

with Max 30100 Sensor. Journal of Applied Electrical & Science Technology. 4(2): 75-80.

[19] U. A. Contardi, M. Morikawa, B. Brunelli and D. V. Thomaz. 2022. MAX30102 Photometric Biosensor Coupled to ESP32-Webserver Capabilities for Continuous Point of Care Oxygen Saturation and Heartrate Monitoring. Engineering Proceedings. 16(1): 1-5.

[20] A. C. Bento. 2020. An Experimental Survey with NodeMCU12e+Shield with Tft Nextion and MAX30102 Sensor. 2020 11th IEEE Annual Information Technology, Electronics and Mobile Communication Conference (IEMCON), Vancouver, BC, Canada. pp. 0082-0086.

[21] P. Foltýnek, M. Babiuch and P. Šuránek. 2019. Measurement and data processing from Internet of Things modules by dual-core application using ESP32 board. Measurement and Control. 52(7-8): 970-984.

[22] J. Vourvoulakis and L. Bilalis. 2021. Real-time pulse oximetry extraction using a lightweight algorithm and a task pipeline scheme. 2021 10th International Conference on Modern Circuits and Systems Technologies (MOCAST), Thessaloniki, Greece. pp. 1-5.

[23] J. R. Camargo L., C. A. Perdomo and O. D. Flórez-Cediel. 2021. Automatic Counting People System as a Strategy to Control Covid-19 Spread. ARPN Journal of Engineering and Applied Sciences. 16(16): 1701-1706.

[24] L. Chong Jin, R. Yusop and D. Ratnadurai. 2020. Autonomous Solar Panels Dry Cleaning System for Dust Removal using Microcontroller and Sensors. International Journal of Advanced Science and Technology. 29(1): 141-152.

[25] C. Navaneethan and S. Meenatchi. 2019. Water Level Monitoring using Blynk Application in IoT. International Journal of Recent Technology and Engineering. 8(4): 1676-1679.

[26] F. H. Cárdenas-Santamaría, M. Ardüa-Flórez, J. M. Jaramillo-Mejía, V. Echeverry-Restrepo, L. A. García-Gutiérrez and A. L. Londoño-Francob. 2018. Arterial blood gas in young adults at an average altitude of 1605-m above sea level: Armenia, Colombia 2016. Colombian Journal of Anestesiology. 46(3): 222-227.

[27] J. A. Viruez-Soto, F. Jiménez-Torres, V. Sirpa-Choquehuanca, R. Casas-Mamani, M. Medina-Vera and O. Vera-Carrasco. 2020. Gasometría Arterial en Residentes a Gran Altura, El Alto - Bolivia 2020. Revista Cuadernos. 61(1): 38-43.

[28] S. I. Sayeed, S. Handoo, H. A. Wani, N. M. Walvir, Q. Danish and R. Pampori. 2015. Arterial blood gas levels in high altitude Kashmiri population, India. International Journal of Research in Medical Sciences. 3(1): 3283-3287.